Efficient Electron Transfer in i-Motif DNA with a Tetraplex Structure

ARTICLE *in* ANGEWANDTE CHEMIE INTERNATIONAL EDITION · DECEMBER 2013

Impact Factor: 11.26 · DOI: 10.1002/anie.201306017 · Source: PubMed

5 AUTHORS, INCLUDING:

Jungkweon Choi

49 PUBLICATIONS **925** CITATIONS

SEE PROFILE

Dae Won Cho

Korea University

106 PUBLICATIONS **1,398** CITATIONS

SEE PROFILE

Bio-nanotechnology

DOI: 10.1002/anie.201306017

Efficient Electron Transfer in i-Motif DNA with a Tetraplex Structure**

Jungkweon Choi, Atsushi Tanaka, Dae Won Cho, Mamoru Fujitsuka, and Tetsuro Majima**

The oxidation and reduction of DNA is closely related to the damage of DNA and the repair of damaged DNA, respectively. DNA has been also regarded as an excellent material for developing DNA-based molecular electronic devices because of its ability as electron carrier and its electrical conductance. Thus, understanding DNA-mediated charge transfer is a prerequisite for the application of DNA in biomedical science and bio-nanotechnology. DNA-mediated charge transfer has been extensively studied by theory and experiments.[1] However, most studies on DNA-mediated charge transfer have focused on the oxidative hole transfer in DNA, whereas relatively few studies have been done on reductive electron transfer.

Generally, DNA-mediated hole transfer occurs over a distance longer than 200 Å[2] and hole transfer along DNA involves many steps of short-distance charge transfer between stacked guanine (G) bases because G among the four natural DNA bases is most sensitive to oxidation.[3] The hole transfer rate depends on the inserted nucleobase between G-C base pairs. In addition, delocalization of the charge over the stacked G bases along the DNA stem has been reported. Meanwhile, the distance for transfer of an excess electron is shorter than that for a hole in DNA. Recently, our group confirmed that an excess electron can migrate over 34 Å through base pairs[4] and the hopping rate of the excess electron among consecutive thymines (T) is faster than the hole trapping rate among adenines (A) and Gs.[5] Furthermore, we showed that single-step electron transfer (through a superexchange mechanism) between a donor (D) in the singlet excited state and an acceptor (A) efficiently occurs and depends on the D-A distance in the nicked-dumbbell DNA sequence.[5]

DNA-mediated electron transfer by a superexchange mechanism occurs dominantly in DNA sequences with one to three base pairs between D and A, whereas charge transfer by the hopping mechanism takes place in a DNA sequence with a long D-A distance. In this study, we investigated the electron transfer in i-motif DNA using fluorescence up-conversion and transient absorption spectroscopic measurements. The i-motif DNA, which is formed from cytosine (C)-rich sequences at slightly acidic pH, has a tetraplex structure formed by the antiparallel intercalation of two parallel hemiprotonated C:C$^+$ base-paired duplexes[6] (Figure 1).

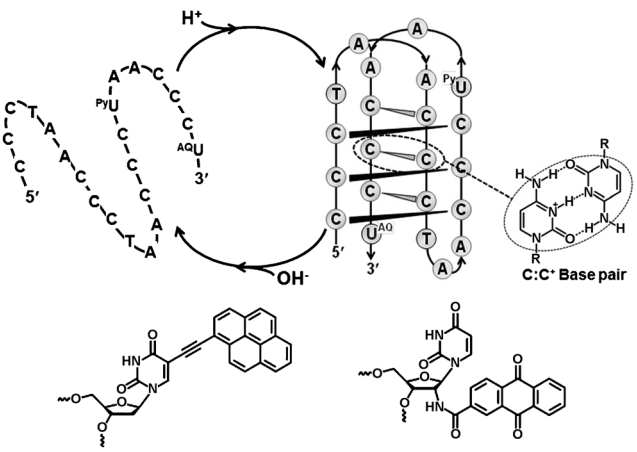

Py-C≡C-dU (^{Py}U) AQ-dU (^{AQ}U)

	Structure	Sequences
i-motif-0	Tetraplex	5′-CCCTAACCCTAACCC- TAACCC- T-3′
Py-i-motif	Tetraplex	5′-CCCTAACCCTAACCC-^{Py}UAA CCC- T-3′
Py-i-motif-AQ	Tetraplex	5′-CCCTAACCCTAACCC-^{Py}UAA CCC-^{AQ}U-3′
Py-dsDNA-AQ	Duplex	5′-CCCTAACCCTAACCC-^{Py}UAA CCC-^{AQ}U-3′ 3′-GGGATTGGGATTGGG- ATTGGG-5′

Figure 1. The reversible pH-induced conformational change of i-motif DNA (Py-i-motif-AQ) used in this study. Py and AQ are used as D and A, respectively.

Recently, i-motif DNA was considered as promising material for application in nanotechnology, for example as a nano-electronic device, because of its reversible pH-induced conformational change as depicted in Figure 1.[7] Especially, this structural change between an extended structure (ssDNA) and a compact structure (i-motif) can be used as a reversible electronic switch. To the best of our knowledge, however, electron transfer occurring in i-motif DNA has not been studied.

[*] Dr. J. Choi, A. Tanaka, Dr. M. Fujitsuka, Prof. Dr. T. Majima
The Institute of Scientific and Industrial Research (SANKEN)
Osaka University, Mihogaoka 8-1, Ibaraki
Osaka 567-0047 (Japan)
E-mail: jkchoi@sanken.osaka-u.ac.jp
majima@sanken.osaka-u.ac.jp
Dr. D. W. Cho
Department of Advanced Materials Chemistry
Korea University
Sejong Campus, Sejong 339-700 (Korea)

[**] This work has been partly supported by the Innovative Project for Advanced Instruments, Renovation Center of Instruments for Science Education and Technology, Osaka University, a Grant-in-Aid for Scientific Research from the Ministry of Education, Culture, Sports, Sciences and Technology (MEXT) of the Japanese Government (grant numbers 25220806, 24550188, 25220806, and 24550188). T.M. thanks to World Class University program funded by the Ministry of Education, Science and Technology through the National Research Foundation of Korea (grant numberR31-2011-000-10035-0) for the support.

Supporting information for this article is available on the WWW under http://dx.doi.org/10.1002/anie.201306017.

For studying electron transfer in i-motif DNA, we used the modified human telomeric sequence (5′-$(CCCTAA)_2CCC$-^{Py}UAA CCC-^{AQ}U-3′, Py-i-motif-AQ). Pyrene (Py) and anthraquinone (AQ) are used as D and A, respectively (Figure 1). In the present study, we clarified the electron transfer occurring in i-motif DNA conjugated with Py and AQ. The result provided herein clearly shows that direct electron transfer from Py in the singlet excited state (^{1}Py*) to AQ in the i-motif rapidly occurs with a rate constant of $6.9\times10^{11}\ s^{-1}$, whereas the electron injection yielding the contact ion pair (CIP) state takes place with a rate constant of $4.0\times10^{11}\ s^{-1}$. Electron transfer between ^{1}Py* and AQ occurs more efficiently in the i-motif than in the duplex DNA because of the compact structure of the i-motif. This is the first report for the photoinduced electron transfer in the i-motif with a tetraplex structure.

Figure 2a shows the circular dichroism (CD) spectrum of Py-i-motif-AQ measured in 100 mM sodium phosphate buffer (pH 5.2). The formation of i-motif from the synthesized oligonucleotide was ensured by its characteristic CD spectrum, producing a positive band at 286 nm and a negative band at 252 nm. The CD spectrum of Py-i-motif-AQ was coincident with that of i-motif-0 measured in pH 4.8 (Figure S2). Moreover, this result is consistent with the results reported by Li et al.,[8] suggesting that the formation and structure of the i-motif is unaffected by the attachment of Py and AQ. The melting temperature (T_m) of Py-i-motif-AQ in pH 5.2 buffer was determined to be 315.4 ± 0.1 K, whereas the T_m of i-motif-0 was determined to be 318.0 ± 0.1 K under the same experimental conditions (Figure S3). Although the T_m value of Py-i-motif-AQ was similar to that of i-motif-0, we found that the structure was slightly destabilized by the covalent attachment of Py. Substantially, the Gibbs free-energy change ($\Delta G=-11.7\pm0.2\ kJ\,mol^{-1}$) for Py-i-motif-AQ at 25 °C is slightly smaller than that of i-motif-0 ($-13.9\pm0.2\ kJ\,mol^{-1}$). Recently, in the study for the i-motif folding process using the 5′-$(CCCTAA)_3CCC$-3′ sequence, Lieblein et al. reported that the kinetically favored minor conformation (3′E) is initially stabilized by stacking interactions and then refolds into a major conformation (5′E) that is stabilized by an extra T-T base pair.[9] Considering their results, we speculate that the destabilization of Py-i-motif-AQ compared to i-motif-0 attributes to the weak T-T base pair by replacing T with 5-(pyrenylethynyl)-2′-deoxyuridine (Py-C≡C-dU). Indeed, Py in the i-motif showed a relatively red-shifted emission band compared to those bands in single-stranded DNA and duplex DNA (Figure S4), indicating that Py in Py-i-motif-AQ DNA is exposed to solvent because of a steric hindrance. Consequently, the extra T-T base pair in Py-i-motif-AQ becomes weakened compared with that in i-motif-0, resulting in the destabilization of Py-i-motif-AQ.

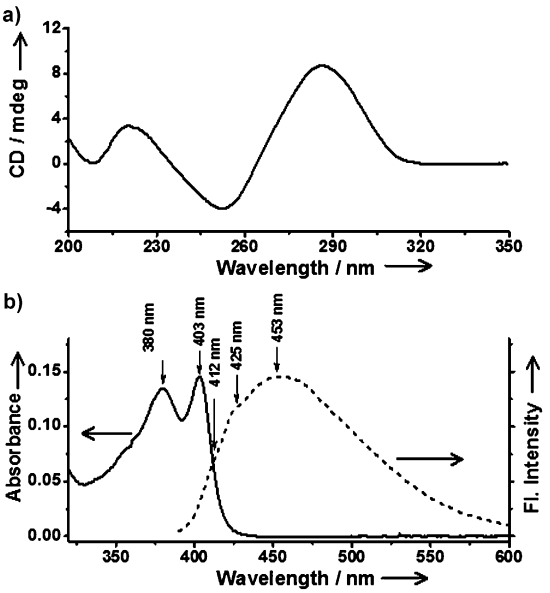

Figure 2. a) Circular dichroism (CD) spectrum of Py-i-motif-AQ measured in 100 mM sodium phosphate buffer (pH 5.2). b) Absorption and emission spectra of Py-i-motif-AQ measured in 100 mM sodium phosphate buffer (pH 5.2; $\lambda_{Ex}=380$ nm; Fl. = fluorescence).

The steady-state fluorescence spectrum of Py-i-motif-AQ showed broad and structured emission bands at 412, 425, and wavelengths longer than 453 nm (Figure 2b). The research groups of Netzel and Wagenknecht reported that ^{Py}U with an ethynyl linker (Py-C≡C-dU) shows a mixed emission spectrum because of ^{1}Py* and a CIP state ($Py^{\bullet+}$-C≡C-$dU^{\bullet-}$).[10] According to their studies, thus, the slightly structured emissions at 412 and 425 nm for Py-i-motif-AQ attribute mainly to ^{1}Py*, whereas the broader emission at wavelengths longer than 453 nm is assigned to the CIP state, which is formed because of a strong electronic coupling between Py and the deoxyuridine (dU) moiety. To confirm the existence of two emissive states observed from Py-i-motif-AQ, the fluorescence up-conversion technique was used to measure the emission lifetime of Py-i-motif-AQ in 100 mM sodium phosphate buffer (pH 5.2). As shown in Figure 3, two emission decay profiles of Py-i-motif-AQ monitored at 460 and 480 nm were fitted by a double-exponential function with two relaxation times of 0.9 ± 0.2 ps ($1.11\times10^{12}\ s^{-1}$) and 9.4 ± 2.4 ps. Meanwhile, Py-i-motif showed the longer decay times than Py-i-motif-AQ (1.4 ± 0.4 ps ($7.1\pm1.6\times10^{11}\ s^{-1}$) and 14.5 ± 7.3 ps), although the difference in two emission decay times for Py-i-motif and Py-i-motif-AQ is small. These results indicate that emissions measured from Py-i-motif and Py-i-motif-AQ attribute to two emissive states, ^{1}Py* and the charge-separated (CS) state. The relative amplitude of the slow-decay component increased when the monitoring wavelength was increased (Table S1 and Figure S5), indicating that the fast- and slow-decay components are assigned to the ^{1}Py* and CS states, respectively.

Interestingly, at the same optical density of all DNA sequences at 400 nm, the emission of Py-i-motif-AQ in acidic solutions was significantly quenched compared with the emissions of Py-ssDNA and Py-i-motif measured in neutral and acidic pH solutions (Figure S4). These results indicate that a different electron-transfer process occurs in the Py-i-motif-AQ sequence in addition to the electron transfer within the Py-dU moiety yielding the CIP state. Considering the singlet excitation energy (E_{00} of about 3.1 eV) of ^{1}Py* in the ^{Py}U nucleotide conjugate, the driving force ($\Delta G_{Py\text{-}AQ}$) of the intramolecular electron transfer from ^{1}Py* to AQ is estimated

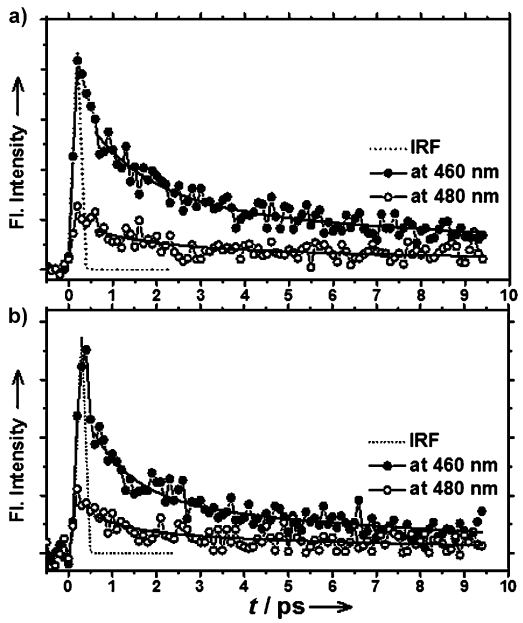

Figure 3. Fluorescence decay profiles of Py-i-motif (top) and Py-i-motif-AQ (bottom) monitored at 460 (black) and 480 nm (blue) with $\lambda_{Ex}=400$ nm in 100 mM sodium phosphate buffer (pH 5.2) measured by the fluorescence up-conversion technique. Theoretical fitting curves are shown as black solid line. Residuals and amplitudes of global fitting results for Py-i-motif and Py-i-motif-AQ are shown in Table S1 and Figure S5 (IRF = instrument response function; Fl. = fluorescence).

to be $\Delta G_{Py\text{-}AQ}=-0.91$ eV using the reported reduction potential of -0.64 V for AQ.[11] The negative value of $\Delta G_{Py\text{-}AQ}$ means that the electron transfer from ^{1}Py* to AQ in i-motif can efficiently occur. Considering the negative value of $\Delta G_{Py\text{-}AQ}$, thus, it is suggested that the fluorescence quenching observed for Py-i-motif-AQ is due to the formation of the CS state through the electron transfer from ^{1}Py* to AQ in i-motif DNA.

To further elucidate the electron-transfer mechanism occurring in i-motif DNA, we measured the femtosecond-transient absorption spectra for Py-i-motif and Py-i-motif-AQ at 100 mM sodium phosphate buffers (pH 5.2). The transient absorption spectrum of Py-i-motif DNA observed after the 400 nm laser excitation consisted of positive signals at about 510, 600, and longer than 700 nm regions, and a negative signal in the wavelength range shorter than 450 nm (Figure 4a). According to studies of the Wagenknecht research group for pyrene-1-yl-2′-deoxyuridine- (Py-dU-) substituted DNA, strong absorption peaks at about 510 and 600 nm attribute to the CIP state ($Py^{\bullet+}$-$dU^{\bullet-}$) formed by electron transfer from ^{1}Py* to dU, and the absorption band with a maximum around 700 nm is assigned to ^{1}(Py-C≡C-dU)*.[1h,12] They suggested that the Py radical cation ($Py^{\bullet+}$) and U radical anion ($dU^{\bullet-}$) in the CIP state reveal strong and broad absorption spectral signatures because of a strong electronic coupling between $Py^{\bullet+}$ and $dU^{\bullet-}$. Thus, we suggest that the positive absorption signal at wavelengths longer than 675 nm is assigned to the formation and decay of ^{1}(Py-C≡C-dU)*, whereas a negative signal at wavelengths shorter than 450 nm attributes to the stimulated emission of Py. In contrast to Py-i-motif, Py-i-motif-AQ showed only positive signals at about 510, 600, and longer than 670 nm wavelengths without any negative signal as depicted in Figure 4b. Especially, upon labeling of AQ to Py-i-motif, the negative signal observed at <450 nm for Py-i-motif was converted to the positive signal in Py-i-motif-AQ, supporting that AQ is involved in the electron transfer occurring in i-motif DNA. Lewis et al. showed that the radical anion of the AQ derivative, N-(hydroxypropyl)anthraquinone-carboxamide, displays weak bands centered at 406 and 575 nm in 100 mM phosphate buffer (pH 7.2).[1e] The research group of Wagenknecht revealed that $Py^{\bullet+}$ exhibits transient absorption band around 475 nm.[1h,12a] Therefore, the positive signal around 450 nm observed for Py-i-motif-AQ may be assigned to $AQ^{\bullet-}$ or $Py^{\bullet+}$. As explained above, however, the positive signal around 450 nm was observed only for Py-i-motif-AQ but not for Py-i-motif. Thus, we suggest that the positive signal at wavelengths shorter than 450 nm observed for Py-i-motif-AQ is assigned to $AQ^{\bullet-}$.

Here, we consider the CS processes occurring in i-motif DNA. First, in Py-i-motif-AQ, the CS state, $Py^{\bullet+}\cdots AQ^{\bullet-}$, can be formed through two processes: direct electron transfer from ^{1}Py* to AQ (superexchange mechanism) and electron transfer from $dU^{\bullet-}$ in the CIP state to AQ by a hopping mechanism. Using pyrene-1-yl-2′-deoxyuridine (Py-dU) substituted DNA, the research group of Wagenknecht showed that most conformers undergo intramolecular electron transfer from ^{1}Py* to dU to form $Py^{\bullet+}$-$dU^{\bullet-}$ within a few picoseconds and that only $dT^{\bullet-}$ (or $dU^{\bullet-}$) but not $dC^{\bullet-}$ can participate as an intermediate charge carrier for the excess electron transfer in DNA.[1h,12b,13] Furthermore, they also suggested that the protonated $dC^{\bullet-}$ can interrupt the excess electron transfer in DNA. Considering results reported by the

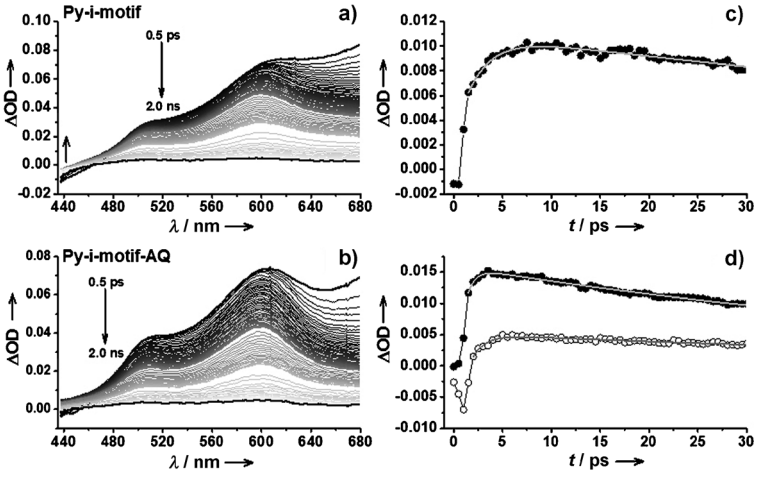

Figure 4. Transient absorption spectra observed after 400 nm laser excitation during femtosecond-laser flash photolysis of a) Py-i-motif and b) Py-i-motif-AQ in 100 mM sodium phosphate buffer (pH 5.2) in the time range of 0.5 ps to 2030 ps at room temperature, respectively (OD = optical density). c) Decay profile of Py-i-motif monitored at 475 nm. d) Decay profiles of Py-i-motif-AQ monitored at 440 (○) and 475 nm (●). Theoretical fitting curves are shown in gray. Residuals for the fitting results for Py-i-motif and Py-i-motif-AQ are shown in Figure S6.

research group of Wagenknecht, therefore, the CS state cannot be formed by electron transfer from $dU^{\bullet-}$ in the CIP state to AQ because of the hemiprotonated C:C$^+$ base pairs of i-motif DNA. Consequently, we conclude that the CS state is formed by direct electron transfer from ^{1}Py* to AQ. The rate constant for the superexchange process (k_s) in Py-i-motif-AQ was directly determined from the rise profile of the absorption band at 440 nm corresponding to $AQ^{\bullet-}$ to be $k_s = 6.9 \pm 1.0 \times 10^{11}\ s^{-1}$ (Figure 4d). Considering the distance dependence on the rate constant for the superexchange process (k_s), the observed k_s value for i-motif DNA, which has three consecutive C:C+ base pairs embedded between D and A (Figure 1), is distinctly large. Indeed, Park et al. showed that the electron transfer occurs at the rate constants of $(3.5–1.8) \times 10^{11}\ s^{-1}$ in the nicked-dumbbell DNA sequences with one to four base pairs between D and A.[14] Lewis et al. reported rate constants of 1.7×10^8–$3.7 \times 10^{10}\ s^{-1}$ for the bridge-mediated electron transfer in hairpin DNA sequences.[15] Although the rate constant for the electron transfer in DNA strongly depends on the kind of photosensitizing chromophore, the rate constant measured in the present study ($k_s = 6.9 \times 10^{11}\ s^{-1}$) is distinctly larger than those reported in several previous studies.[5,14,15] This indicates that the direct electron transfer from ^{1}Py* to AQ in i-motif DNA occurs faster than in a duplex DNA including hairpin DNA. Moreover, Py-dsDNA-AQ at pH 7.0 did not show a positive absorption signal in the wavelength range shorter than 450 nm, indicating that the electron transfer from ^{1}Py* to AQ in a duplex DNA does not take place (data not shown). Comparing two structures of i-motif and duplex DNA, i-motif DNA has less consecutive base pairs embedded between D and A than the duplex DNA; five consecutive base pairs (two A-T and three G-C base pairs) for a duplex DNA and three consecutive C:C$^+$ base pairs for i-motif DNA. Furthermore, it is known that the stacking distance between C:C$^+$ base pairs in i-motif DNA is 3.1 Å,[6d] whereas the distance between two bases in dsDNA is 3.4 Å. Therefore, the structural change from dsDNA (or ssDNA) to i-motif results in a significant decrease in the D-A distance. On these grounds, we conclude that the fast electron transfer observed in i-motif DNA ($k_s = 6.9 \times 10^{11}\ s^{-1}$) did not result from electron transfer from $dU^{\bullet-}$ in the CIP state but from the direct electron transfer from ^{1}Py* to AQ because of the hemiprotonated C:C$^+$ base pairs as well as the relatively compact structure of i-motif.

The generation rate of $Py^{\bullet+}$ ($k_{Py^{\bullet+}}$) in Py-i-motif-AQ was estimated to be $k_{Py^{\bullet+}} = 1.05 \pm 0.28 \times 10^{12}\ s^{-1}$ from the rise profile of the absorption band at 475 nm corresponding to $Py^{\bullet+}$ (Figure 4d). This value is larger than that measured for Py-C≡C-dU-substituted DNA molecules ($3.3–5.0 \times 10^{11}\ s^{-1}$).[1h] As shown in Figure 5, the generation of $Py^{\bullet+}$ can be attributed to two pathways, that is, the electron injection yielding the CIP state and electron transfer from ^{1}Py* to AQ with rate constants of k_{CIP} and k_s, respectively. Therefore, $k_{Py^{\bullet+}}$ is the sum of k_{CIP} and k_s, $k_{Py^{\bullet+}} = k_{CIP} + k_s$, resulting in a large $k_{Py^{\bullet+}}$. Furthermore, $k_{Py^{\bullet+}}$ of $1.05 \times 10^{12}\ s^{-1}$ is well consistent with the ^{1}Py* lifetime of Py-i-motif-AQ determined by the fluorescence up-conversion technique.

To accurately determine k_{CIP} in i-motif DNA, we measured the formation time of the CIP state by electron transfer from ^{1}Py* using Py-i-motif, which shows only the electron injection process yielding the CIP state. From analysis of the time profile at 475 nm (Figure 4c) $k_{CIP} = 4.0 \pm 0.4 \times 10^{11}\ s^{-1}$ was determined for Py-i-motif to be close to the ^{1}Py* lifetime of the Py-i-motif as shown by fluorescence up-conversion within the experimental error. This value is also consistent with that reported by the research group of Wagenknecht.[1h] Based on the determined k_{CIP} and k_s values, $k_{Py^{\bullet+}}$ of $1.09 \times 10^{12}\ s^{-1}$ was calculated for Py-i-motif-AQ to be well consistent with the experimentally determined $k_{Py^{\bullet+}} = 1.05 \times 10^{12}\ s^{-1}$. This consistency supports that $k_{Py^{\bullet+}}$ determined in the present study is very reasonable value for the generation rate of $Py^{\bullet+}$ in Py-i-motif-AQ and that no excess electron transfer occurs from $dU^{\bullet-}$ in the CIP state to AQ but the direct electron transfer occurs efficiently from ^{1}Py* to AQ in i-motif DNA.

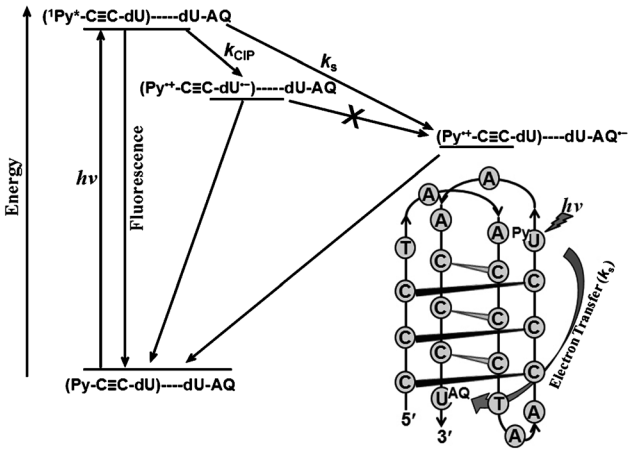

Figure 5. Energy diagram for the photoinduced electron transfer in Py-i-motif-AQ DNA.

Molecular electronic devices incorporating i-motif DNA have been developed for nano-biotechnological applications because of the pH-induced reversible conformational change of i-motif DNA. In this regard, we studied the electron transfer in i-motif DNA conjugated with Py and AQ as D and A, respectively, in acidic solutions. The results clearly show that the direct electron transfer from ^{1}Py* to AQ in i-motif DNA with a tetraplex structure occurs at $k_s = 6.9 \times 10^{11}\ s^{-1}$, whereas the electron injection yielding the CIP state takes place at $k_{CIP} = 4.0 \times 10^{11}\ s^{-1}$. However, the direct electron transfer from ^{1}Py* to AQ does not take place in a duplex DNA in neutral solutions, indicating that the fast electron transfer from ^{1}Py* to AQ (superexchange mechanism) in i-motif DNA with $k_{Py^{\bullet+}} = 1.05 \times 10^{12}\ s^{-1}$ is due to the hemiprotonated C:C$^+$ base pairs as well as its compact structure. No excess electron transfer occurs from $dU^{\bullet-}$ in the CIP state to AQ. The result provided herein reveals that i-motif DNA is a good electron carrier and that its structural change between ssDNA (or dsDNA) and i-motif is expected as a reversible electronic switch in nanoelectronic devices.

Received: July 11, 2013
Revised: September 11, 2013
Published online: November 4, 2013

Keywords: charge separation · electron transfer · fluorescence up-conversion · DNA · molecular devices

[1] a) J. D. Slinker, N. B. Muren, S. E. Renfrew, J. K. Barton, *Nat. Chem.* **2011**, *3*, 228 – 233; b) H. A. Wagenknecht, *Nat. Prod. Rep.* **2006**, *23*, 973 – 1006; c) M. Fujitsuka, T. Majima, *J. Phys. Chem. Lett.* **2011**, *2*, 2965 – 2971; d) N. Renaud, Y. A. Berlin, F. D. Lewis, M. A. Ratner, *J. Am. Chem. Soc.* **2013**, *135*, 3953 – 3963; e) F. D. Lewis, A. K. Thazhathveetil, T. A. Zeidan, J. Vura-Weis, M. R. Wasielewski, *J. Am. Chem. Soc.* **2010**, *132*, 444 – 445; f) P. Daublain, A. K. Thazhathveetil, Q. Wang, A. Trifonov, T. Fiebig, F. D. Lewis, *J. Am. Chem. Soc.* **2009**, *131*, 16790 – 16797; g) M. J. Park, M. Fujitsuka, H. Nishitera, K. Kawai, T. Majima, *Chem. Commun.* **2012**, *48*, 11008 – 11010; h) P. Kaden, E. Mayer-Enthart, A. Trifonov, T. Fiebig, H. A. Wagenknecht, *Angew. Chem.* **2005**, *117*, 1662 – 1666; *Angew. Chem. Int. Ed.* **2005**, *44*, 1636 – 1639; i) M. Tanaka, K. Oguma, Y. Saito, I. Saito, *Chem. Commun.* **2012**, *48*, 9394 – 9396.

[2] a) B. Giese, *Annu. Rev. Biochem.* **2002**, *71*, 51 – 70; b) G. B. Schuster, *Acc. Chem. Res.* **2000**, *33*, 253 – 260; c) T. Takada, K. Kawai, M. Fujitsuka, T. Majima, *Proc. Natl. Acad. Sci. USA* **2004**, *101*, 14002 – 14006.

[3] a) E. Meggers, M. E. Michel-Beyerle, B. Giese, *J. Am. Chem. Soc.* **1998**, *120*, 12950 – 12955; b) K. Nakatani, C. Dohno, I. Saito, *J. Am. Chem. Soc.* **1999**, *121*, 10854 – 10855; c) F. D. Lewis, J. Q. Liu, X. B. Zuo, R. T. Hayes, M. R. Wasielewski, *J. Am. Chem. Soc.* **2003**, *125*, 4850 – 4861; d) Y. Osakada, K. Kawai, M. Fujitsuka, T. Majima, *Proc. Natl. Acad. Sci. USA* **2006**, *103*, 18072 – 18076; e) J. Choi, J. Park, A. Tanaka, M. J. Park, Y. J. Jang, M. Fujitsuka, S. K. Kim, T. Majima, *Angew. Chem.* **2013**, *125*, 1172 – 1176; *Angew. Chem. Int. Ed.* **2013**, *52*, 1134 – 1138.

[4] K. Tainaka, M. Fujitsuka, T. Takada, K. Kawai, T. Majima, *J. Phys. Chem. B* **2010**, *114*, 14657 – 14663.

[5] M. J. Park, M. Fujitsuka, K. Kawai, T. Majima, *J. Am. Chem. Soc.* **2011**, *133*, 15320 – 15323.

[6] a) M. Guéron, J. L. Leroy, *Curr. Opin. Struct. Biol.* **2000**, *10*, 326 – 331; b) J. Choi, T. Majima, *Chem. Soc. Rev.* **2011**, *40*, 5893 – 5909; c) J. Choi, S. Kim, T. Tachikawa, M. Fujitsuka, T. Majima, *J. Am. Chem. Soc.* **2011**, *133*, 16146 – 16153; d) L. Chen, L. Cai, X. Zhang, A. Rich, *Biochemistry* **1994**, *33*, 13540 – 13546.

[7] J. Choi, T. Majima, *Photochem. Photobiol.* **2013**, *89*, 513 – 522.

[8] X. Li, Y. Peng, J. Ren, X. Qu, *Proc. Natl. Acad. Sci. USA* **2006**, *103*, 19658 – 19663.

[9] A. L. Lieblein, J. Buck, K. Schlepckow, B. Furtig, H. Schwalbe, *Angew. Chem.* **2012**, *124*, 255 – 259; *Angew. Chem. Int. Ed.* **2012**, *51*, 250 – 253.

[10] a) S. T. Gaballah, G. Collier, T. L. Netzel, *J. Phys. Chem. B* **2005**, *109*, 12175 – 12181; b) S. T. Gaballah, Y. H. A. Hussein, N. Anderson, T. T. Lian, T. L. Netzel, *J. Phys. Chem. A* **2005**, *109*, 10832 – 10845; c) E. Mayer, L. Valis, C. Wagner, M. Rist, N. Amann, H. A. Wagenknecht, *ChemBioChem* **2004**, *5*, 865 – 868; d) M. Rist, N. Amann, H.-A. Wagenknecht, *Eur. J. Org. Chem.* **2003**, 2498 – 2504.

[11] H. J. van Ramesdonk, B. H. Bakker, M. M. Groeneveld, J. W. Verhoeven, B. D. Allen, J. P. Rostron, A. Harriman, *J. Phys. Chem. A* **2006**, *110*, 13145 – 13150.

[12] a) N. Amann, E. Pandurski, T. Fiebig, H. A. Wagenknecht, *Chem. Eur. J.* **2002**, *8*, 4877 – 4883; b) M. Raytchev, E. Mayer, N. Amann, H. A. Wagenknecht, T. Fiebig, *ChemPhysChem* **2004**, *5*, 706 – 712; c) A. Trifonov, M. Raytchev, I. Buchvarov, M. Rist, J. Barbaric, H. A. Wagenknecht, T. Fiebig, *J. Phys. Chem. B* **2005**, *109*, 19490 – 19495.

[13] N. Amann, E. Pandurski, T. Fiebig, H. A. Wagenknecht, *Angew. Chem.* **2002**, *114*, 3084 – 3087; *Angew. Chem. Int. Ed.* **2002**, *41*, 2978 – 2980.

[14] M. J. Park, M. Fujitsuka, K. Kawai, T. Majima, *Chem. Eur. J.* **2012**, *18*, 2056 – 2062.

[15] F. D. Lewis, R. S. Kalgutkar, Y. S. Wu, X. Y. Liu, J. Q. Liu, R. T. Hayes, S. E. Miller, M. R. Wasielewski, *J. Am. Chem. Soc.* **2000**, *122*, 12346 – 12351.

